

Proceedings

# Theoretical Study of the Aza-Wittig Reaction, $\text{Me}_3\text{P}=\text{NR}$ (R = Methyl or Phenyl) with Aldehyde by the DFT and DFT-D Methods (Dispersion Correction)

†

A. ADDA <sup>1,2</sup> and et H. SEDIKI <sup>1,3</sup>

<sup>1</sup> LCPM, Chemistry Department, Faculty of Sciences, University of Oran 1, Ahmed Benbella, Es-Senia, Oran 31000, Algeria; adda20052000@yahoo.fr

<sup>2</sup> Research Centre in Analytical Chemistry and Physics (CRAPC), BP 248, Algiers RP, Algiers 16004, Algeria

<sup>3</sup> Department of Materials Technology, Faculty of Physics, University of Science and Technology Mohamed Boudiaf, Oran 31000, Algeria

† Presented at the 24th International Electronic Conference on Synthetic Organic Chemistry, 15 November–15 December 2020; Available online: <https://ecsoc-24.sciforum.net/>.

Received: date; Accepted: date; Published: date

**Abstract:** The Aza-Wittig reaction played an important role in organic transformations and has known considerable development in the construction of cyclic and acyclic compounds in neutral solvents in the absence of catalysts with a high yield of products. Today, the use of iminophosphoranes (Phosphazenes) has become a powerful tool in organic synthesis strategies directed towards the construction of nitrogenous heterocycles. These can react with carbonyl compounds, an excellent method for the construction of C=N double bonds via intermolecular and intramolecular Aza-Wittig reactions. In this study, we are interested in the theoretical study of the reaction path of the Aza-Wittig reaction between trimethyl-iminophosphoranes  $(\text{CH}_3)_3\text{P}=\text{NR}$ , R =  $\text{CH}_3$  or Ph) for the two-substituent methyl and phenyl with Acetaldehyde, including continuum solvation. Our calculations were carried out by means of ab-initio calculations using the theory of DFT and DFT-D, dispersion correction term using the Grimme method in the program Gaussian09, using the functional B3LYP and B3LYP-GD3BJ with a 6-31G\*\* base. The results obtained allowed us to highlight the mechanisms of the Aza-Wittig reaction in particular after the addition of the term of dispersion correction or Van der Walls correction which provided a new description of this reaction and its chemical path.

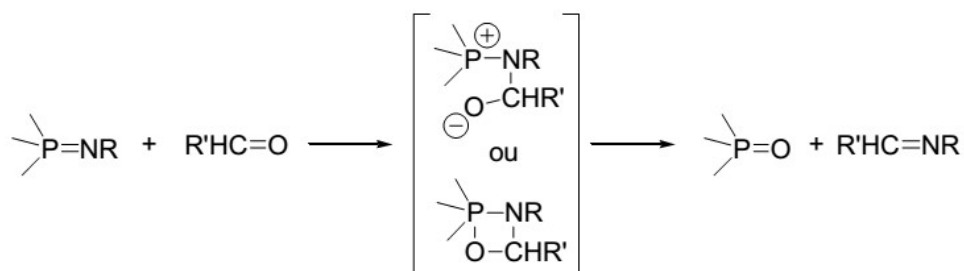
**Keywords:** Aza-Wittig; phosphazenes; trimethyl-iminophosphoranes; DFT; dispersion correction; Van der Walls correction

## 1. Introduction

Phosphazenes (iminophosphoranes) of the simple structure  $\text{R}_3\text{P}=\text{NR}'$  were first described by Staudinger and Meyer in 1919 [1] but their applications only began in the 1950s. There are different names to designate this chemical function P=N in particular: iminophosphorane, phosphinimine,  $\lambda$ -phosphazene or phosphinimide.

However, compared to extensive studies of the Wittig reaction [2–11], little attention has been paid to the Aza-Wittig reaction. In 1997, JugoKoketsu and colleagues [18] first investigated the Aza-Wittig reaction of iminopnictoranes ( $\text{H}_3\text{NMH}$ , M = P, As, Sb and Bi) with formaldehyde ( $\text{H}_2\text{CO}$ ) at the MP2 level. They came to the conclusion that the Aza-Wittig reaction was more favorable for Phosphorus for As, Sb and Bi.

The Aza-wittig reaction is arguably the most important reaction in the iminophosphorane reactivity panel. To elucidate the mechanism of Aza-Wittig reactions, it is important to isolate their intermediates, although such isolations are generally difficult due to their instability. This reaction consists of a nucleophilic attack of the iminophosphoranes on the carbonyl (or thio-carbonyl) derivatives, followed by the removal of phosphine oxide (or phosphine sulfide). This reactivity very clearly resembles that of phosphorus ylides (Scheme 1), hence its name.



**Scheme 1.** Scheme showing two possible paths of the Aza-Wittig reaction mechanism.

The mechanism of the Aza-Wittig reaction is broadly known; we know in particular that it has two stages with fairly similar speeds. On the other hand, little experimental data is available on the intermediates (Betaine or Oxazaphosphetidine) of the reaction path, even if some special cases have been studied and characterized [12,13]

The greatest advances in the mechanism of the Aza-Wittig reaction have been made by theoretical studies of the reaction path by post Hartree-Fock methods such as: Møller-Plesset at orders 2 and 4 and DFT [14–16]

As part of this work, we have studied the reaction of Aza-Wittig for the two substituents of R, methyl and phenyl  $(\text{CH}_3)_3\text{P}=\text{NR}$  with Acetaldehyde ( $\text{C}_2\text{H}_4\text{O}$ ) Figure 1. However, to our knowledge, no theoretical study on the DFT-D calculation (Van der Waals dispersion correction) has yet been published on the Aza-Wittig reaction. The present work can provide theoretical information on this reaction.

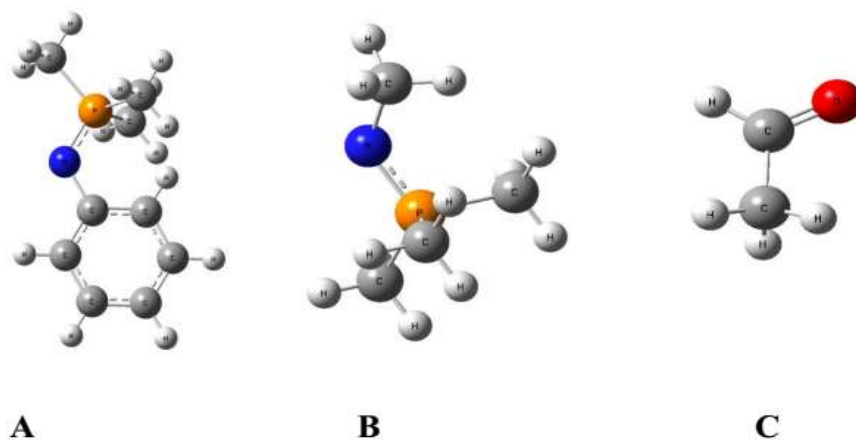


**Figure 1.** Optimized geometries of the reagents used in the Aza-Wittig reaction mechanism with A, B and C represent phosphazene with phenyl, phosphazene with methyl and Acetaldehyde respectively.

## 2. Computational Methods

All the calculations reported in this paper have been performed within density functional theory using the functional B3LYP [17–19] and B3LYP-GD3BJ (Empirical dispersion) with a base 6-31G\*\* [20]. Each point of the reaction path is fully optimized and verified to be a transition state (TSX) with

imaginary frequency or stable species with real frequencies (i.e., RC reagents, intermediate INX and PC products). Frequency analysis is performed to obtain thermochemical information about the reaction processes at 298 K. All calculations are performed using the Gaussian-09 program, and the resulting surfaces were visualized using GaussView 6. IRC (Intrinsic Reaction Coordinate) calculations were also performed to confirm the nature of the transition states.

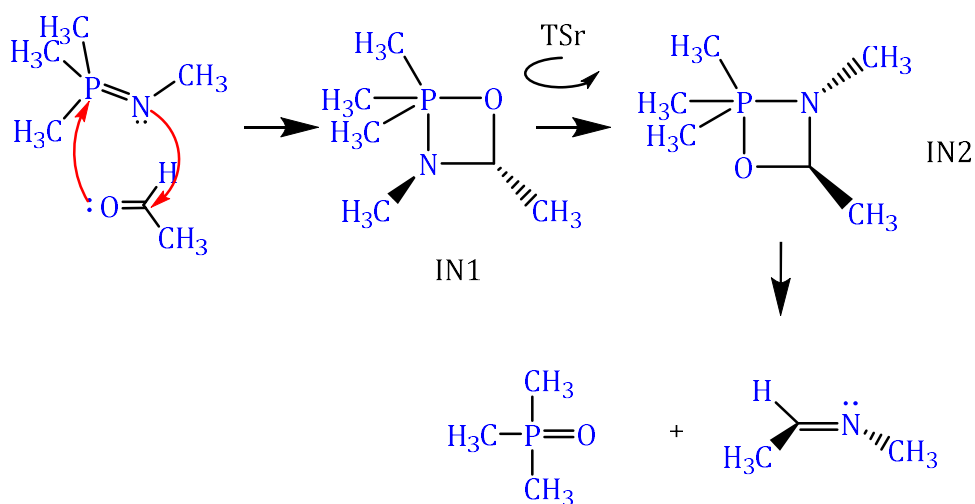
Single point energy calculations have also been carried out for all species involved in the reaction at gas phase B3LYP-GD3BJ/6-31G\*\* optimized geometries in THF (tetrahydrofuran) solvent using integral equation formalism polarizable continuum model (IEFPCM).

### 3. Results and Discussion

#### 3.1. Reaction of Methylimino(trimethyl)phosphorane with Acetaldehyde

Using DFT calculations at B3LYP/6-31G\*\* and B3LYP-GD3BJ/6-31G\*\* level, it is shown that the reaction of the Aza-Wittig continues through  $(\text{CH}_3)_3\text{P}=\text{NCH}_3 + \text{O}=\text{CH}_2\text{CH}_3 \rightarrow \text{RC} \rightarrow \text{TS1} \rightarrow \text{IN1} \rightarrow \text{TSr} \rightarrow \text{IN2} \rightarrow \text{TS2} \rightarrow \text{PC} \rightarrow (\text{CH}_3)_3\text{P}=\text{O} + \text{CH}_3\text{N}=\text{CH}_2\text{CH}_3$  where RC and PC represents a reactive and product complex, TS represents a transition state and IN an intermediate state.

In our work, we have found that the Aza-Wittig reaction between Iminophosphorane and aldehyde is strongly exothermic and involves a stable [2+2] Cycloaddition-Cycloreversion sequence, with two intermediates IN1 and IN2 (Figure 2).



**Scheme 2.** mechanism of Aza-Wittig reaction (methylimino(trimethyl)phosphorane with Acetaldehyde).

The first TS1 transition structure is located at only 10.44 and 8.73 kcal/mol, for B3LYP and B3LYP-D3, above the reactants which corresponds to a supra-supra geometry. This first Cycloaddition [2+2] turns out to be quite asynchronous (Table 1), with a calculated synchronicity of 0.93 and 0.94. This observation is consistent with the analysis performed by McEwen for the similarity reaction of Wittig on the binding order using a semi-empirical method, which showed that the new C–C bond is formed at about 40% in the TS, while the P–O binding is still negligible at this stage [21,22]. The addition barrier is high in B3LYP functional compared to the addition barrier in B3LYP-D3, after incorporation of dispersion corrections.

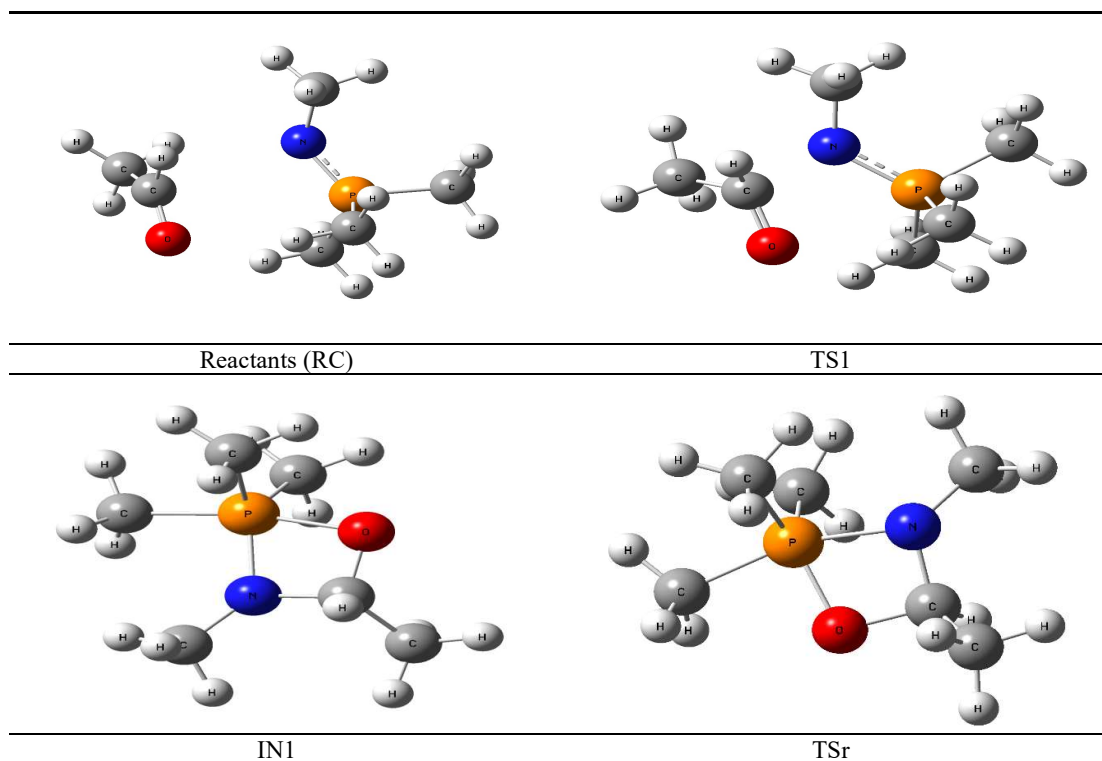
**Table 1.** Bond lengths (in Å) and dihedral angles (in degrees) of the Aza-Wittig reaction of methylimino(trimethyl)phosphorane with Acetaldehyde ( $(\text{CH}_3)_3\text{P}=\text{NCH}_3$ ).

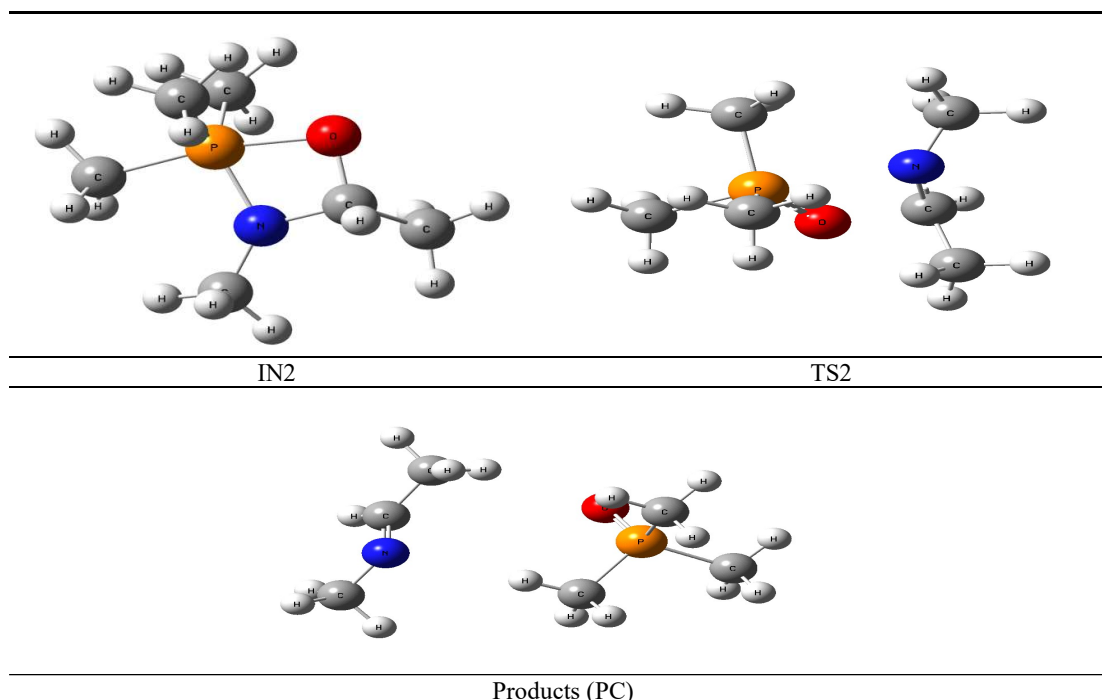
B3LYP/6-31G**	$d_{\text{P-N}}$	$d_{\text{C-O}}$	$d_{\text{P-O}}$	$d_{\text{N-C}}$	$\Phi_{\text{PNCO}}$
B3LYP-D3/6-31G**	Ångström	Ångström	Ångström	Ångström	
<i>Reactants (RC)</i>	1.58	1.22	3.63	3.07	-2.42
	1.58	1.22	3.45	2.84	-0.50
<i>TS1</i>	1.64	1.28	2.69	1.76	-7.30
	1.63	1.28	2.70	1.76	-6.75
<i>IN 1</i>	1.72	1.40	1.84	1.47	-6.73
	1.71	1.40	1.84	1.46	-6.95
<i>TSr</i>	1.81	1.42	1.73	1.45	-11.76
	1.81	1.43	1.73	1.45	-11.66
<i>IN2</i>	1.72	1.40	1.84	1.47	-6.75
	1.71	1.40	1.84	1.46	-6.95
<i>TS2</i>	2.42	1.69	1.59	1.36	8.58
	2.41	1.69	1.59	1.36	10.20
<i>Products (PC)</i>	4.13	3.76	1.51	1.27	-2.11
	3.89	3.53	1.51	1.27	-2.01

We have also found an IN1 reaction intermediate of Oxazaphosphetidine, in which the P=O bond is 1.84. Our results also indicate that IN2 is a fairly stable reaction intermediate.

In the intermediary of IN1, the coordination geometry around phosphorus is approximately a Trigonal bipyramid, with oxygen derived from the aldehyde group found at the apical position. This then undergoes pseudo-rotation on a low barrier to give an IN2 isomer with the Iminophosphorane nitrogen in the apical position (IN2) Table 2.

**Table 2.** Optimized geometries of structures involved in the reaction pathway.





The IRC calculations performed for the 3 TSs (TS1, TSr, TS2) show that the localized TSs are well connected to the intermediates and final products. Indeed, optimizing the geometry of the last structure obtained on the IRC curve in the intermediate direction to IN1, IN2 and products give a structure identical to the intermediate IN1, IN2 and final product.

**Table 3.** Relative energies, enthalpy and Gibbs free energy (kcal/mol) calculated by the DFT, at the Table 3. LYP and B3LYP-D3 with a base of 6-31G\*\*. (D: Dispersion corrections of Grimme).

Structures	(B3LYP)			(B3LYP-D3)		
	$\Delta E$ (kcal/mol)	$\Delta G$ (kcal/mol)	$\Delta H$ (kcal/mol)	$\Delta E$ (kcal/mol)	$\Delta G$ (kcal/mol)	$\Delta H$ (kcal/mol)
Reactants (RC)	0.00	0.00	0.00	0.00	0.00	0.00
TS1	10.44	14.77	10.28	8.73	12.17	8.52
IN 1	-6.63	-0.05	-5.01	-8.23	-2.46	-6.62
TSr	-0.71	6.44	-0.98	-3.63	2.75	-2.85
IN2	-6.63	-0.05	-5.01	-8.23	-2.46	-6.62
TS2	12.75	17.97	12.80	11.20	16.06	11.32
Products (PC)	-30.27	-29.31	-29.53	-27.94	-26.90	-27.15

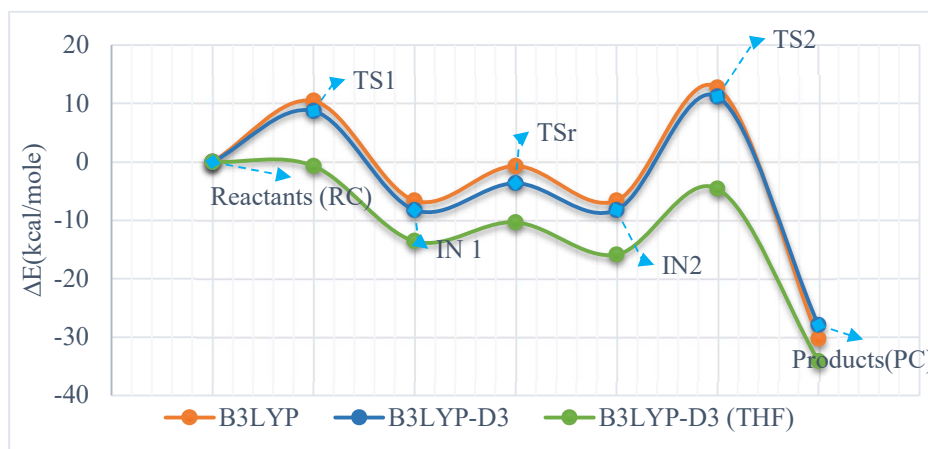


**Figure 2.** Potential energy diagram of the reaction of Aza-Wittig of Methylimino(trimethyl) phosphorane with Acetaldehyde in gas phase B3LYP, B3LYP-D3 and with solvent B3LYP-D3 (THF).

The Cycloreversion step [2+2] of the reaction takes place from IN2 to TS2 and has an activation energy greater than that calculated for the first step in Table 4, the incorporation of dispersion correction in functional B3LYP decreases the energy of activation corresponds to Cycloaddition-Cycloreversion of Oxazaphosphetidine. Regarding the effects on the molecular structure of the products are minor, this difference is explained by the emergence of a dipole-dipole interaction between the two reagents at the addition. Note that the addition of the dispersion correction in the Hamiltonian more precisely in the exchange and correlation equation, for the functional B3LYP, slightly stabilized the structures of intermediates, cycloaddition. Thus, the addition process is more favored kinetically.

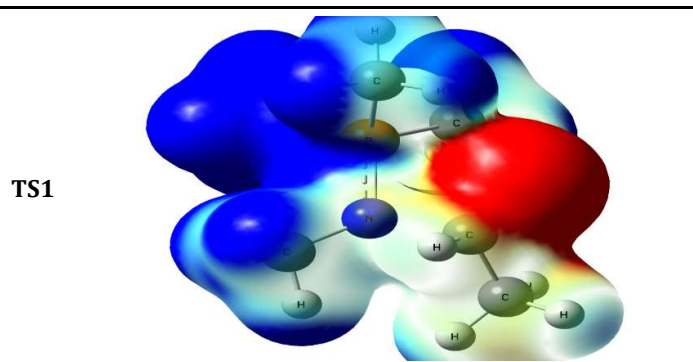
On the other hand, for the energy calculation including dispersion correction, B3LYP-D3/6-31G\*\* (THF) seems to underestimate the energy barriers by  $-0.69$  kcal/mol compared to that calculated at B3LYP-D3/6-31G\*\*. The energy values for the addition steps with addition of solvent and dispersion correction are estimated to be  $-13.57$  kcal/mol. Lower energy barriers suggest that the inclusion of dispersion correction and solvent have a significant effect on the reaction. For the second stages, the energy values are  $-15.86$  kcal/mol.

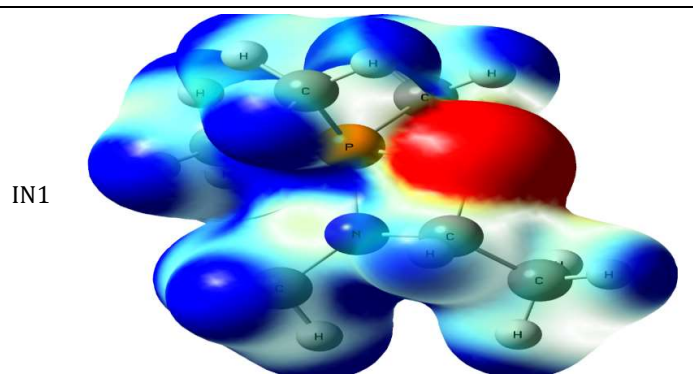
**Table 4.** Activation energy corresponds to Cycloaddition-Cycloreversion of Oxazaphosphetidine for Figure 3. LYP, B3LYP-D3.

	$\Delta G_{B3LYP}^\ddagger$	$\Delta G_{B3LYP-D}^\ddagger$
RC $\rightarrow$ TS1	14.77	12.17
IN2 $\rightarrow$ TS2	18.01	18.52

Table 5 shows that negatively charge Iminophosphorane nitrogen is attracted to the carbon atom of the positive charge aldehyde in TS1 because there is a wide region of negative electrostatic potential around the nitrogen atom which confirms the negative charge in the carbon, this charge decreases in the intermediates Oxazaphosphetidine IN1. These potential electrostatic surfaces also support the initial stages of the reaction path in which a nucleophilic attack of nitrogen against the carbon aldehyde occurs.

**Table 5.** Maps of total electron density, calculated electrostatic potential for TS1 and intermediates IN1, regions of highest electron density distribution are displayed in intense red  $-16.31$  kcal/mol and regions of density distribution lower electronics in intense blue  $+16.31$  kcal/mol.





### 3.2. Reaction of Phenylimino(trimethyl)phosphorane with Acetaldehyde

Geometric data and relative energies corresponding to the reaction of Phenylimino (trimethyl) phosphorane ((CH<sub>3</sub>)<sub>3</sub>P=NPh) with Acetaldehyde (CH<sub>3</sub>C=O) at B3LYP and B3LYP-D3/6-31G\*\* are given in Tables 6 and 8 respectively.

**Table 6.** Bond lengths (in Å) and dihedral angles (in degrees) of the Aza-Wittig reaction of methylimino(trimethyl)phosphorane with Acetaldehyde (CH<sub>3</sub>)<sub>3</sub>P=NPh.

B3LYP/6-31G**	<i>d<sub>P-N</sub></i>	<i>d<sub>C-O</sub></i>	<i>d<sub>P-O</sub></i>	<i>d<sub>N-C</sub></i>	$\Phi_{\text{PNCO}}$
B3LYP-D3/6-31G**	Ångström	Ångström	Ångström	Ångström	
<i>Reactants (RC)</i>	1.59	1.22	3.60	3.12	-3.38
	1.59	1.22	3.46	2.89	0.72
<i>TS1</i>	1.65	1.29	2.55	1.74	-7.29
	1.64	1.29	2.57	1.73	-8.33
<i>IN 1</i>	1.73	1.40	1.84	1.47	-5.42
	1.72	1.40	1.84	1.47	-5.35
<i>TSr</i>	1.93	1.45	1.68	1.44	-4.88
	1.91	1.45	1.68	1.43	-5.37
<i>IN2</i>	1.92	1.44	1.68	1.44	-3.55
	1.90	1.44	1.69	1.44	-3.71
<i>TS2</i>	2.60	1.62	1.59	1.38	1.77
	2.50	1.58	1.60	1.39	8.90
<i>Products (PC)</i>	4.05	3.21	1.51	1.28	9.05
	3.75	2.97	1.51	1.28	11.62

The first transition state TS has an almost planar structure TS1, in which the dihedral angle  $\Phi_{\text{PNCO}}$  = -7.29 and -8.33 (for B3LYP-D3), for the second transition state TS2 takes the values of  $\Phi_{\text{PNCO}}$  = 1.77 and 8.90. As shown in Figure 3 the second TS barrier is lower compared to TS1, this may explain kinetically that the reaction with phenyl as a substituent in the Aza-Wittig reaction is more stable and the reaction takes place rapidly in the second elimination step, Cycloreversion, of imine. Therefore, the Aza-Wittig reaction of the can be much more kinetically favorable for CH<sub>3</sub> in the first Cycloaddition step and less favorable in the Cycloreversion step on the contrary in the case where the phenyl substituent is bonded in Imionphosphrane, with regard to the thermodynamic stability reaction with CH<sub>3</sub> and more favored over phenyl.



**Table 7.** Optimized geometries of structures involved in the reaction pathway.

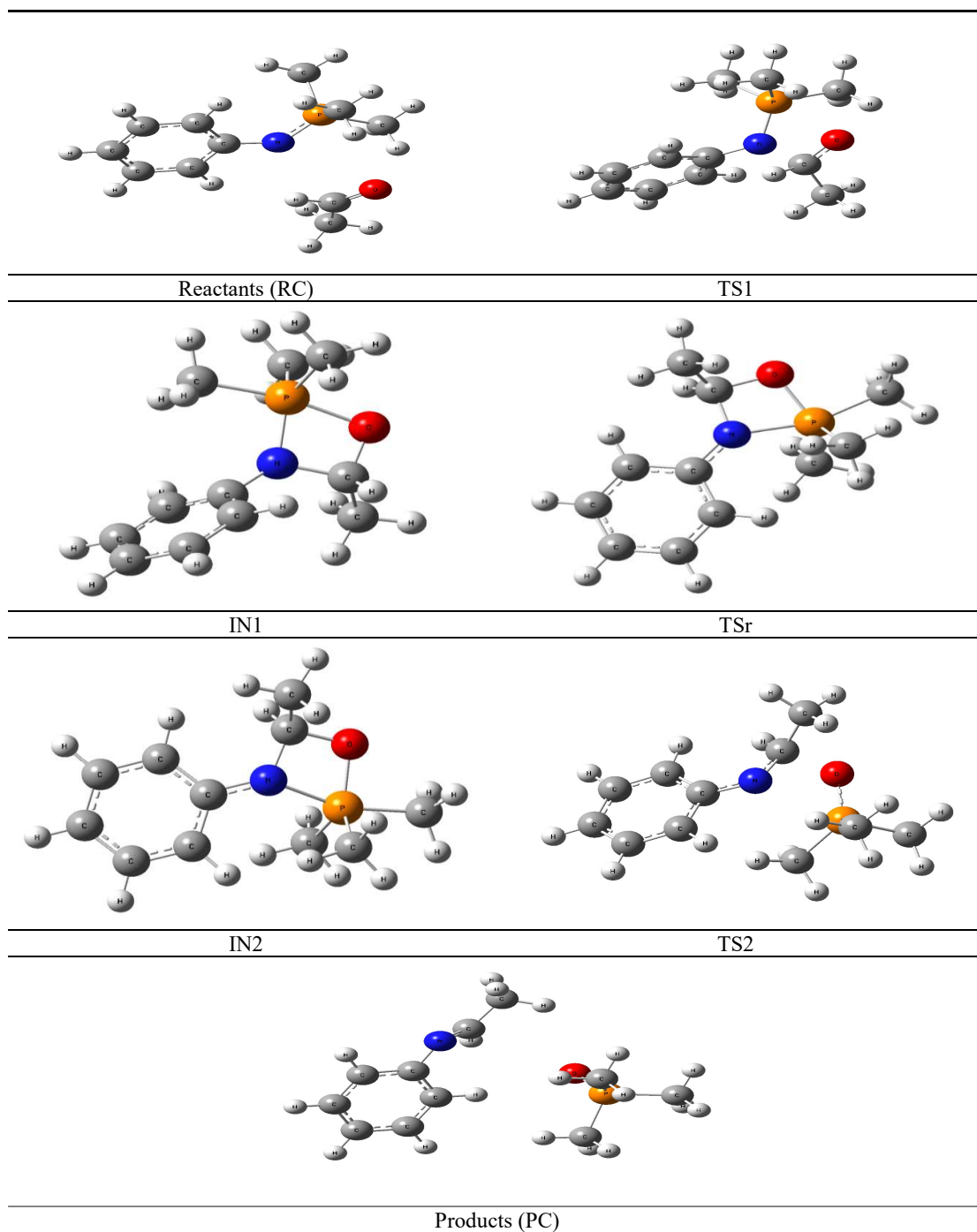


**Table 8.** Relative energies, enthalpy and Gibbs free energy (kcal/mol) calculated by the DFT, at the theoretical level B3LYP and B3LYP-D3 with a base of 6-31G\*\*.

Structures	(B3LYP)			(B3LYP-D3)		
	$\Delta E$ (kcal/mol)	$\Delta G$ (kcal/mol)	$\Delta H$ (kcal/mol)	$\Delta E$ (kcal/mol)	$\Delta G$ (kcal/mol)	$\Delta H$ (kcal/mol)
<i>Reactants (RC)</i>	0	0	0	0.00	0.00	0.00
<i>TS1</i>	15.88	19.05	15.59	13.76	16.30	13.40
<i>IN 1</i>	1.69	7.36	3.03	-0.11	3.69	1.15
<i>TSr</i>	2.18	9.21	3.00	0.23	6.08	0.99
<i>IN2</i>	0.66	7.51	2.15	-1.30	4.37	0.14



<b>TS2</b>	10.23	14.87	10.24	8.85	13.31	8.98
<b>Products (PC)</b>	-24.35	-23.29	-23.67	-22.55	-21.48	-21.89

Relative Energies, Enthalpy and Free Energy for intermediates and transition states are more stable for functional B3LYP-D3 compared to B3LYP, without dispersion correction. Neglect of dispersion correction with solvent appears to lead to a huge overestimate the activation barriers by single point at B3LYP-D3/6-31G\*\*(THF). Thus, inclusion of dispersion correction significantly lowers the activation barriers for reaction (see Figure 3).

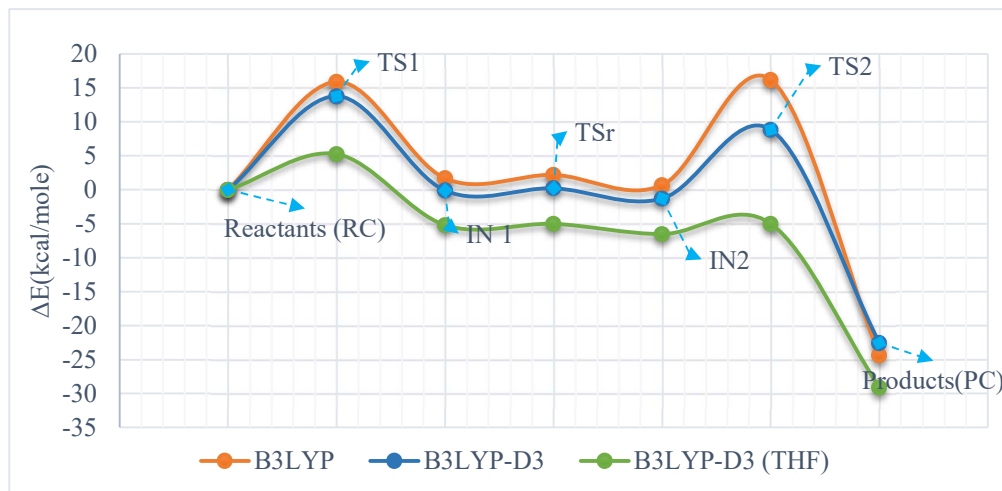


**Figure 3.** Potential energy diagram of the reaction of Aza-Wittig of Phenylimino(trimethyl) phosphorane with Acetaldehyde in gas phase B3LYP, B3LYP-D3 and with solvent B3LYP-D3 (THF).

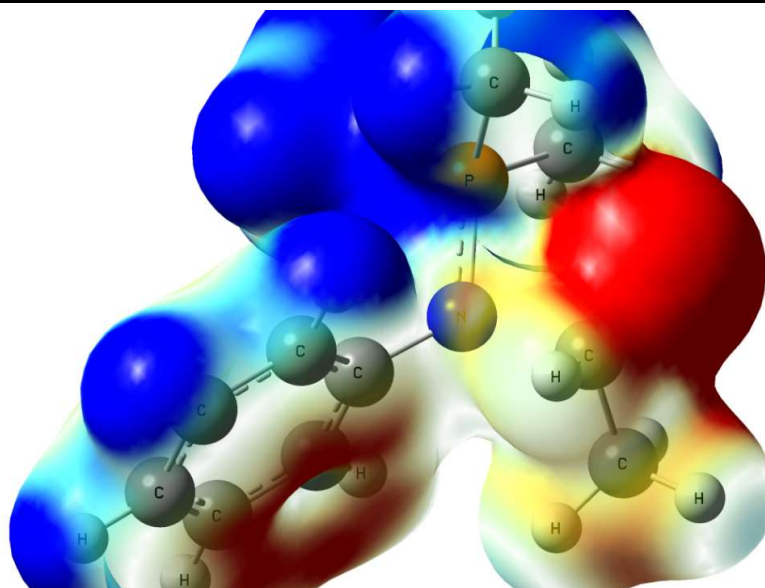
**Table 9.** Activation energy corresponds to Cycloaddition-Cycloreversion of Oxazaphosphetidine for functional B3LYP, B3LYP-D3.

	$\Delta G_{B3LYP}^\ddagger$	$\Delta G_{B3LYP-D}^\ddagger$
RC → TS1	19.05	16.30
IN2 → TS2	7.35	8.93

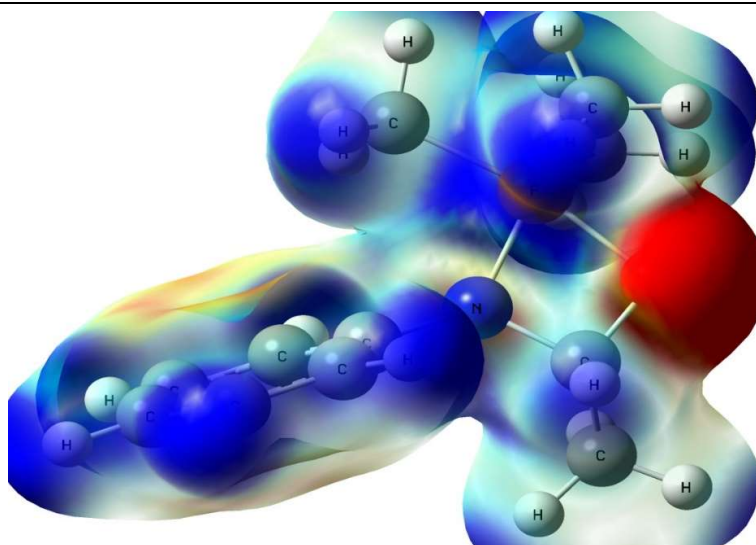
Table 10 shows that negative charge Iminophosphorane nitrogen is attracted to the positive charge of the carbon atom of aldehyde in TS1, because there is a wide region of negative electrostatic potential around the nitrogen atom which confirms the negative charge in the carbon, this charge decreases in the intermediates Oxazaphosphetidine IN1. These potential electrostatic surfaces also support the initial stages of the reaction path in which a nucleophile attack of nitrogen against the carbon aldehyde occurs.

**Table 10.** Maps of total electron density, calculated electrostatic potential for TS1 and intermediates IN1, regions of highest electron density distribution are displayed in intense red -16.31 kcal/mol and regions of density distribution lower electronics in intense blue +16.31 kcal/mol.

TS1



IN1



#### 4. Conclusions

The aza-wittig reaction of trimethyliminophosphorane ( $(\text{CH}_3)_3\text{P}=\text{NR}$ ) for both methyl and phenyl substituents was investigated by means of ab-initio calculations by DFT and DFT-D (dispersion correction) on the basis of 6-31G\*\*. We conclude in this study that: The aza-Wittig reaction between phosphazenes and aldehydes takes place by a [2+2] Cycloaddition-Cycloreversion mechanism, with Oxazaphosphetidines being the reaction intermediates. The two processes [2+2] are associated with thermally authorized asynchronous processes.

Methylimino(trimethyl)phosphorane is more reactive than phenylimino(trimethyl)phosphorane and less reactive in the second stage of elimination, Cycloreversion, of imine. Intermediate Oxazaphosphetidines are four membered rings in which the nitrogen atom is pyramidal. However, the energy barriers associated with the rotational movement are localized between the two intermediates, therefore, only the second stage leading to the imines and phosphine oxides. The addition of the term dispersion correction brings a new description of the reaction and the path of the chemical reaction, because it makes it possible to find a better description of the dispersion interactions in the description of the corrected functions and of the DFT method

**Acknowledgments:** The authors are deeply grateful to the University of Oran (Algeria) for computing resources and computer time used on Haytham at the UCI (Unité de Calcul Intensif), and to the University of Reims Champagne Ardennes (URCA, France) for computing resources and computer time used on Romeo calculator and Al-Farabi Cluster computer of the Ecole Nationale Polytechnique Oran—Maurice Audin.

## References

1. Staudinger, H.; Meyer, J. On New Organic Phosphorus Bonding. *Helv. Chim. Acta* **1919**, *2*, 612–618.
2. Natio, T.; Nagase, S.; Yamataka, H.J. *Am. Chem. Soc.* **1994**, *116*, 10080.
3. Volatron, F.; Einstein, O.J. *Am. Chem. Soc.* **1987**, *109*, 1.
4. Streitwieser, A.; Rajca, A.; McDowell, R.S.; Glaser, R.J. *J. Am. Chem. Soc.* **1987**, *109*, 4184.
5. Dixon, D.A.; Smart, B.E. *J. Am. Chem. Soc.* **1986**, *108*, 172.
6. Eades, R.A.; Gassman, P.G.; Dixon, D.A. *J. Am. Chem. Soc.* **1983**, *103*, 1066.
7. Vincent, M.A.; Schaefer, H.F.; Schier, A.; Schmidbaur, H.J. *J. Am. Chem. Soc.* **1983**, *105*, 3806.
8. Holler, R.; Lischka, H.J. *Am. Chem. Soc.* **1980**, *102*, 4632.
9. Maryanoff, B.E.; Raitz, A.B. *Chem. Rev.* **1989**, *89*, 863.
10. Lischka, H.J. *Am. Chem. Soc.* **1977**, *99*, 353.
11. Nguyen, M.T.; Hegarty, A.F. *J. Chem. Soc. Perkin Trans.* **1987**, *2*, 47.
12. Bachrach, S.M. *J. Org. Chem.* **1992**, *57*, 4367.
13. Sasaki, T.; Egushi, S.; Okano, T.J. *Am. Chem. Soc.* **1983**, *105*, 5912–5913.
14. Sheldrick, W.S.; Schomburg, D.; Schmidpeter, A.; von Criegern, T. *Chem. Ber.* **1980**, *113*, 55.
15. Molina, P.; Alajarin, M.; Leonardo, C.L.; Claramunt, R.M.; Focesfoces, M.D.; Cano, F.H.; Catalan, J.; Depaz, J.L.G.; Elguero, J.J. *Am. Chem. Soc.* **1989**, *111*, 355–363. Lu, W.C.; Liu, C.B.; Sun, C.C. *J. Phys. Chem. A* **1999**, *103*, 1078–1083.
16. Lu, W.C.; Sun, C.C.; Zang, Q.J.; Liu, C.B. *Chem. Phys. Lett.* **1999**, *311*, 491–498.
17. Koketsu, J.; Ninomiya, Y.; Suzuki, Y.; Koga, N. *Inorg. Chem.* **1997**, *36*, 694–702.
18. Becke, A.D. Density-Functional Exchange-Energy Approximation with Correct Asymptotic Behavior. *Phys. Rev. A* **1988**, *38*, 3098.
19. Lee, C.; Yang, W.; Parr, R.G. Development of the Colle-Salvetti correlation-energy formula into a functional of the electron density. *Phys. Rev. B* **1988**, *37*, 785.
20. Hariharan, P.C.; Pople, J.A. The Influence of Polarization Functions on Molecular Orbital Hydrogenation Energies. *Theor. Chem. Acc. Theory, Comput. Modeling (Theor. Chim. Acta)* **1973**, *28*, 213–222.
21. Mari, F.; Lahti, P.K.; McEwen, W.E. *Heteroat. Chem.* **1991**, *2*, 265–276.
22. Mari, F.; Lahti, P.K.; McEwen, W.E.J. *Am. Chem. Soc.* **1992**, *114*, 813–821.

**Publisher's Note:** MDPI stays neutral with regard to jurisdictional claims in published maps and institutional affiliations.



© 2020 by the authors. Licensee MDPI, Basel, Switzerland. This article is an open access article distributed under the terms and conditions of the Creative Commons Attribution (CC BY) license (<http://creativecommons.org/licenses/by/4.0/>).